Sedimentary Architecture of an Ancient Linear Draa (Barremian, Neuquén Basin): Insights into the Long-Term Development and Evolution of Aeolian Linear Bedforms

Short title: Architecture of Aeolian Linear Bedforms

Agustín Argüello Scotti[1*]

Gonzalo D. Veiga[1]

** - Corresponding author, aarguello@cig.museo.unlp.edu.ar*

[1]Centro de Investigaciones Geológicas (CONICET-Universidad Nacional de La Plata), Diagonal 113 #275 (B1904DPK), La Plata, Argentina.

Abstract

Linear aeolian bedforms are the most abundant bedform type in modern Earth sand seas and are very common in our Solar System. Despite their abundance, the long-term development of these bedforms and its impact upon the resulting sedimentary architecture in the geological record is still poorly understood. The aims of this paper are to study the exposed record of an ancient linear *draa* in order to discuss the factors that impact the development and sedimentary architecture of aeolian linear bedforms. The outcrops of the ancient Troncoso Sand Sea (Barremian, Neuquén Basin, Argentina) provide a unique opportunity to access a preserved *draa* record with an external body geometry that unequivocally confirms its linear morphology. Statistical analysis reveals significant differences for several aspects of cross-bedded set bodies and bounding surfaces within the bedform record and allows for the identification of three architectural complexes. Insights from deterministic models, and analysis of the complexes' internal relative chronology and distribution indicates that architectural complexes result from particular phases in bedform development. It also shows that the construction of this *draa* was characterized by expansion from a core, where the oldest deposits are located, and that its development was characterized by sustained growth and strong longitudinal behaviour, triggering bedform evolution though different configurations. Factors that impact the development and architecture of linear bedforms are identified and discussed, and their relative importance in comparison to bedforms of transverse behaviour is evaluated. Finally, a scheme of expected sedimentary architecture styles for linear bedforms is presented. This case study clearly shows how growth can be a critical factor over linear bedform architecture and indicates how the preservation of certain styles of sedimentary architecture may not be as unusual in the geological record as previously thought.

Word count = 286

Keywords = Sedimentary architecture, Aeolian linear bedforms, Bedform development, Cretaceous, Neuquén Basin, Troncoso Inferior

Acknowledgments: This research was funded by the Consejo Nacional de Investigaciones Científicas y Técnicas (CONICET-PIP 112-201101-00322) and through a co-operation agreement between YPF S.A. and the Centro de Investigaciones Geológicas. The authors are also grateful to Nicolás Scivetti and Joaquín Bucher for their valuable assistance in the field, and Nigel P. Mountney, Ernesto Schwarz, Luis A. Spalletti and Bailey A. Lathrop for their encouragement and feedback that though different stages of this study.

Introduction

Linear dunes -relatively symmetric, continuous, simple forms- (Lancaster, 1995; Livingstone and Warren, 1996) and linear *draa* -dunes with superimposed dunes- (Mountney, 2006; Wilson, 1972) are the most abundant bedform type in modern sandy deserts (Lancaster, 1982). In spite of this, establishing the dominant characteristics of the sedimentary architecture associated with these bedforms has been problematic over several decades. The difficulty to access the interior of modern dunes (McKee and Tibbitts, 1964), the apparent scarcity of this dune type in the geological record (Rubin and Hunter, 1985), and open questions about the long-term behaviour of these particularly slow-moving bedforms (Rubin et al., 2008), have made it difficult to record and predict the sedimentary architecture resulting from linear bedform development.

More recently, GPR and OSL techniques on modern dunes have finally allowed the characterization of simple linear dune’s sedimentary architecture and have considerably improved our understanding of their dynamics (Bristow et al., 2007, 2000). However, long-term variability in linear bedform kinematics, scale and shape is still poorly understood, even less how such variables impact the resulting sedimentary architecture in the geological record. Considering that GPR and OSL techniques have depth limitations that hinder studies of larger and older *draa*-scale forms, ancient examples with good quality outcrops can certainly aid in testing models of sedimentary architecture attributed to linear bedforms and provide further insights over their long-term development.

In the geological record, most examples of sedimentary deposits assigned to deposition by linear bedforms seem to fall between two types of sedimentary architecture (Fig. 1). These have been categorized as “lateral migration” and “vertical accretion” models when attributed to particular types of linear *draa* migration (Clemmensen, 1989; Scherer, 2000). Examples from the former category are broadly characterized by unimodal spread of cross-bedding dip-azimuths, oblique to the dip-azimuths of the internal bounding surfaces (Ahmed Benan and Kocurek, 2000; Clemmensen, 1989; Scherer, 2000), and are consistent with lateral migration-dominated theoretical models proposed by Rubin and Hunter (1985). Other ancient examples fall within the latter category and are characterized by a bimodal (not bipolar) distribution of cross-bedding dip-azimuths (Bose et al., 1999; Clemmensen, 1989; Glennie, 1972; Steele, 1983), and are consistent with longitudinal behaviour theoretical models proposed by Rubin and Hunter (1985). Nonetheless, ancient examples with good exposures across an entire bedform and an external body geometry that unequivocally confirms the presence of a linear bedform are yet to be reported.

The aeolian deposits within the Troncoso Inferior Member of the Huitrín Formation (Neuquén Basin, Argentina) are characterized by the exceptional preservation of large- and small-scale bedform morphology (Veiga et al., 2005). Large-scale bedforms of linear morphology have been identified in this ancient aeolian system both in remarkable quality exposures (Argüello Scotti and Veiga, 2015; Strömbäck et al., 2005) and in the subsurface (Dajczgewand et al., 2006). Therefore, the aims of this work are to study the sedimentary architecture within an exceptionally preserved and exposed linear *draa* from the geological record of the Troncoso Inferior Member, obtain a conceptual model of its development, and discuss the factors that impact the development and sedimentary architecture of linear aeolian bedforms.

Concepts and Terminology Used in This Study

Considering that the shape, scale and kinematics of a particular bedform are major parameters that determine its sedimentary architecture (Rubin, 1987), the terminology related to these aspects is briefly discussed for a later consistent use across this paper. It should also be considered that these parameters are also variables, in the sense that bedforms adjust their shape, scale and kinematics to changing environmental controls.

In this paper, the usage of the terms “morphology”, “size” and “dynamics” refers strictly to the shape, scale and kinematics, respectively, of a bedform at a certain time (Table 1). For instance, the usage of the term “linear” bedforms is used strictly as a morphological expression in this study, following Rubin and Hunter (1985). Linear dunes can be found in different scales and shapes, such as *seifs* (Lancaster, 1995; Tsoar, 1982), linear ridges (vegetated linear dunes of Tsoar, 1989; Warren, 2013) and complex or compound linear *draa* (McKee, 1983). Linear bedforms can also be classified according to their dynamics in longitudinal or oblique (*sensu* Rubin and Hunter, 1985), which result from the relative importance of elongation (*sensu* Tsoar et al., 2004) and lateral migration (Bristow et al., 2005; Rubin et al., 2008) processes.

Moreover, the usage of the terms “evolution”, “behaviour” and “growth” is proposed to refer to the changes in the shape, kinematics and scale of a bedform, respectively, over a particular time period (Table 1). In this regard, bedform “development” is referred to as the sum of the changes over those variables (or lack thereof) over a particular time period. Not included in this concept of development are high-frequency autocyclic variations, such as bedform asymmetry cycles controlled by seasonal winds typical of linear dunes,. In the case of large aeolian bedforms, and especially for large aeolian linear bedforms, their development can be described as “long-term” in the sense that it takes place over extended timespans that can seldom be registered from modern examples (e.g. >10^2 y; Rubin et al., 2008).

Geological Setting and Study Area

The Troncoso Inferior Member of the Huitrín Formation (Groeber, 1946) is part of the sedimentary infill of the Neuquén Basin (Howell et al., 2005) (Fig. 2). It is considered to be Barremian in age, constrained by fossil assemblages in underlying and overlying marine units (Aguirre-Urreta et al., 2017; Lazo and Damborenea, 2011, respectively). In the north-eastern sector of the basin, the study unit is characterized by sandstones related to the development of a large dune field or *erg*, overlying sandstones of fluvial/aeolian origin or, in some cases, a variety of sedimentary deposits of marine origin. This erg, known as the Troncoso Sand Sea (Argüello Scotti, 2017), has a preserved extension of over 6000 km^2 and was developed during a period in which the basin was completely disconnected from the proto-Pacific Ocean, being therefore considered as an inland erg. The final morphology of the dune field is partially preserved due to the abrupt marine flooding of the basin and the subsequent deposition of evaporites, as a result from a partial reconnection with the open ocean (Veiga et al., 2005).

The area selected for this study is the Loma La Torre outcrop at the southern Pampa de Tril plain, in the north-western Neuquén Province (Figs. 2, 3). Previous studies in this location (Argüello Scotti and Veiga, 2015) show that large-scale preserved bedforms constitute linear-shaped ridges, oriented WSW-ENE, with a width close to 1 km, a symmetric cross-section, a spacing close to 1.5 km, and a preserved remnant height of 24-30 m. The erg system's record is bounded at the base by planar and subhorizontal sand drift surface (*sensu* Clemmensen and Tirsgaard, 1990), characterized by signs of deflation, and capped at the top by a marine transgressive super surface (*sensu* Havholm and Kocurek, 1994). The system's record completely thins out in the intervening interdune areas, which don't show any indication of water-lain, or even water-influenced, deposition. In other words, the Troncoso Sand Sea record in this locality solely comprises the record of the preserved large-scale bedforms, which constitute this work's study interval. These characteristics indicate a dry aeolian system that did not undergo accumulation (*sensu* Kocurek, 1999) in a relatively marginal erg sector.

The most accessible of the large-scale preserved bedforms at the Loma La Torre outcrop was selected for this study, for which information on the preserved morphology and thickness of the bedform's record are available from previous studies (Fig. 3). The outcrops that comprise the study section offer a continuous two-dimensional cliff section of the preserved bedform´s southern flank, oriented N110°-290° and oblique to bedform orientation (N81°-261°), and a discontinuous but more three-dimensional exposure of its northern flank.

Previous facies analysis of the study interval at this locality (Argüello Scotti and Veiga, 2015; Strömbäck et al., 2005), indicate a low diversity of sedimentary facies, belonging to aeolian and subordinated soft-sediment deformed facies associations. The most characteristic facies are well to moderately sorted, fine- to medium-grained sandstones, with high-angle trough and planar, low-angle, and more rarely, subhorizontal stratification and lamination (Fig. 4A, B). Basic aeolian stratification types characteristic of deposition under a dry sandy substrate are abundant (grainfall laminae, grainflow strata, subcritically climbing translatent strata; Fig. 4B, C), while stratification types under a damp surface (adhesion ripple forms) are extremely uncommon. Soft sediment deformation of aeolian facies is evidenced by structures formed by folding, such as convolute laminae, wavy subparallel bedding, cone-shaped diapirs and broad synclines, and dish structures. These facies are only abundant in the upper sectors of the study interval, and were formed by rapid upwards escape of water and/or air associated with pressure changes within the dunes resulting from flooding (Strömbäck et al., 2005).

Methods

The workflow designed for this study (Fig. 5) is centred on a sedimentary architecture analysis (Kocurek et al., 1991). Field data acquisition (qualitative and quantitative) focused on two key elements of the sedimentary record of the preserved bedform: the cross-stratified set bodies and their bounding surfaces. Characterization of these elements allowed for the definition of contrasting architectural styles, identified as “architectural complexes”, whose internal complexity, distribution and chronology of set bodies was analysed.

Data acquisition and processing

A combination of surveying methods were used to characterize the sedimentary architecture exposed in the outcrops, including (i) ground- and aerial-based photography, (ii) sedimentary logs, and (iii) direct measurements and observations over the accessible parts of the outcrop. Aerial photography was used to build a digital photomosaic over which the inferred sedimentary architecture was mapped, and later confirmed or corrected with field observations, resulting in three architectural panels. From these panels, the shape and position of the individual cross-stratified bodies and bounding surfaces were analysed. The position of each element was established in relation to the morphological features observed in the study section, such as *draa* flank and crest sectors (Fig. 2). Six detailed sedimentary logs were measured across the study section, allowing for grain-size and sorting observations, aeolian stratification types recognition and estimation of their abundance within set bodies, set body thickness measurements, and dip angle and azimuth readings of cross-bedding and bounding surfaces using a Brunton compass. Direct measurements and observations were carried out for all set bodies and intervening bounding surfaces that were accessible by foot, delivering the same information as logs. Specific categories were defined to estimate the relative abundance of aeolian stratification types within set bodies. Criteria used for recognition of aeolian stratification types are the same as in Argüello Scotti and Veiga (2015). The following categories were identified from the relative abundance between wind-ripple laminae (climbing translatent strata of Hunter, 1977) and grainflow strata (Kocurek and Dott, 1981): (i) wind-ripple dominated (no grainflow); (ii) wind-ripple abundant; (iii) wind-ripple/grainflow couplets; (iv) grainflow abundant; (v) grainflow-dominated (no wind-ripple). Grainfall laminae were identified and usually present at all these categories, but they were of little volumetric importance in the section and across the study interval in general. Finally, a virtual outcrop model was generated from ground- and aerial-based photography, following a structure-from-motion workflow. The model was built from approximately 200 photographs, using Visual SFM (Wu, 2011) and MeshLab (Cignoni et al., 2008) software, and was scaled and referenced with data from a total station survey. Using VRGS software (University of Manchester), cross-stratified set body dimensions (maximum thickness and apparent width), and additional measurements of dip angle and azimuth of cross-bedding and bounding surfaces were extracted from the model. The final architectural panels (Fig. 6) combine the information obtained from different sources.

As a result, a total of 70 cross-stratified set bodies were analysed across the study section. The final dataset includes a total of 137 dip-azimuth readings of cross-stratification from 46 set bodies, and a total of 37 dip-azimuth readings from bounding surfaces. Dip-azimuth cross-stratification measurements were averaged for each set body, resulting in what is here referred to as “paleocurrent direction”. In addition, the intra set body variability of cross-bedding dip-azimuth was measured as a strength vector (Collinson et al., 2006) when at least 3 values per body were available.

Data analysis

The architectural complexes defined within the study section are defined by significant differences in several aspects of the set bodies and bounding surfaces, such as maximum thickness, apparent width, paleocurrent and bounding surface orientations and external geometry. Minor differences are also seen in the abundance of aeolian stratification types and textural and compositional aspects of the sandstones. Some of these significant differences were stablished statistically, indicating that the elements within each complex belong to a particular population.

Reconstruction and interpretation of the bedform morphodynamics and development aspects that relate to each complex was assisted by deterministic modelling using

BEDFORMS software (Rubin, 1987). In addition, the distribution of the complexes (i.e., location within the study section, abundance and relative superposition) and the internal relative chronology of their set bodies was inspected. These analyses provided a wealth of information that allowed reconstructing the development of this ancient linear *draa*.

Sedimentary Architecture

Architectural complexes

The sedimentary architecture observed in the study section is separated into three complexes with particular architectural style (Figs. 6, 7, Table 2) and other minor differences (see methods). The architectural style is considered in terms of the dimensions, shape and distribution of set bodies and orientation of both foresets and bounding surfaces. Statistically significant differences between the maximum thickness of set bodies belonging to different complexes were established by Fisher's variance test (ANOVA) at a level of p<0.05 [F (3.64) = 23.36; p<0.0001], and Kruskal-Wallis test also at p<0.05 [H = 40.85; p<0.0001]. Very similarly, significant differences of apparent width data were established by Fisher's variance test (ANOVA) [F (3.48) = 20.25; p<0.0001] and Kruskal-Wallis test [H = 34.79; p<0.0001], always at a level of p<0.05. Tukey's and Dunn's tests for multiple comparisons (Table 3) indicated the specific differences between each population. The differences between complexes (quantitative and qualitative) are demonstrated to be the result of a particular phase in the development of the preserved bedform, indicating that each complex is composed of genetically-related set bodies and bounding surfaces.

Complex 1

Description. Complex 1 is characterized by small cross-bedded set bodies (maximum thickness usually between 1 and 2 m; apparent width around 20 m, Table 2) with a wedge-like geometry (Figs. 6, 8A). The complex occupies a very small area (only 1%) in the bedform section, in which only 7 set bodies can be identified. The set bodies show a higher proportion of clasts of opaque heavy minerals in comparison to the other complexes in the study section (Fig. 8C). Regarding aeolian stratification types, the set bodies of the first complex are usually composed of wind-ripple/grainflow couplets (interbedding between wind-ripple lamination-dominated and grainflow-dominated intervals). Paleocurrent distribution is bimodal, spanning from a 60° to 125° mode to a 320° to 360° mode (Fig. 9). From the few preserved bounding surfaces, two measurements of dip-azimuth were obtained, 120° and 349°. In particular, the oldest set body preserved within this complex is different in some aspects from the rest of the sets of the studied section (Fig. 8A). Texturally, the sandstones that comprise the first set are moderately sorted, having a higher proportion of very fine- and coarse-grained sand in comparison to other complexes. The dominant stratification types in the first set body are wind-ripple lamination and grainfall lamination, and grainflow strata are lacking. Also, a stratum of adhesion ripples (Fig. 8B) is found in this set, the only clear sign of humidity observed in the study section. The dip angle of the cross-bedding in the first set is around 10° towards 340°. Even if this complex was eroded to a great extent before the deposition of the subsequent complex, the remaining record is enough to carry out interpretations.

Interpretation. A bimodal distribution of paleocurrent directions and bounding surface's dip-azimuths, coupled with individual cross-bedding in set bodies dipping oblique to the strike of it associated lower bounding surface and to the largest axis of the set body, is consistent with the architecture expected for a sinuous linear dune with a sustained longitudinal dynamic (dominant elongation, minor lateral migration; Rubin et al., 2008; Figs. 55 and 77 of Rubin, 1987). In this case, each opposing side of the same dune crest is responsible for the formation of set bodies with one of the two paleocurrent modes. The strike of the bounding surfaces and the orientation of the set body's largest axis is sub-parallel to the dunes elongation direction. On the other hand, the texture and stratification types of the oldest preserved set body indicate that its associated original bedform lacked an active slipface and could represent the remains of an incipient bedform like a dome dune.

The spatial relationship between the first set body and the rest of the sets in this complex is similar to which it could be expected from a growing, elongating sinuous linear dune, as seen in Rubin et al. (2008) and the models built for this study (next section) which emulate the behaviour and growth of *seif* dunes. Taking those models into consideration, the first set of the complex is likely the remains of a linear dune tip or nose, later covered by the deposits of the same elongating dune. In this way, the sedimentary architecture of Complex 1 can be explained by the growth (i.e. size increment) and longitudinal behaviour (i.e. sustained longitudinal dynamics) of a single, small linear dune or *seif*.

Complex 2

Description. Complex 2 is characterized by the occurrence of very-large set bodies (maximum thickness average at 4-5 m, and up to 8.5 m; apparent width average at 65-66 m, Table 2, Figs. 6, 8) occupying a large area (around 47%) in the study section. Set bodies in this complex show a clear bimodal paleocurrent and bounding surface dip-azimuth distribution, dependent on the position in the section. A 315° to 15° paleocurrent mode is dominant in the northern flank of the preserved bedform section, while a 45° to 165° mode is dominant in the southern flank (Fig. 9, considering both wedge and trough-shaped set bodies). Bounding surfaces in the flank sectors are planar/tangential in shape and have dip-azimuths from 315° to 0° in the northern flank and from 100 to 150° in the southern flank. In contrast, bounding surfaces in the crest sector are concave upward and have a bimodal dip-azimuth distribution. Furthermore, the large set bodies can also be separated into trough-shaped and wedge-shaped bodies (Table 4, Figs. 6, 8, 9). Trough-shaped bodies (Figs. 8D, 9) are located within the centre of the section, they have a high intra-set body variability of cross-bedding dip-azimuth (low S value, Table 4), and have an acute bimodal paleocurrent distribution. Wedge-shaped bodies (Figs. 8F, 9) are found in the flank areas; they have fairly constant intra-set cross-bedding dip-azimuth (high S value, Table 4) and show an obtuse bimodal paleocurrent distribution. Trough-shaped bodies are dominated by wind-ripple/grainflow couplets (Fig. 8E), whereas wedge-shaped bodies are more abundant in wind-ripple lamination, increasing gradually in importance towards the base of the set and away from the section crest until becoming wind-ripple dominated (Fig. 8G). Towards the top of this complex, very small-scale set bodies (maximum thickness average less than 1 m; apparent width average around 12 m) are found in groups between the large-scale sets, bounded within a trough-shaped lower bounding surface (Figs 6, 8D). They comprise a particular population (Tables 2, 3, Fig. 7), even if they are of little volumetric importance (2% of Complex 2 section).

Interpretation. Very much alike Complex 1, the second complex's large trough-shaped bodies found at the bedform centre, characterized by a bimodal paleocurrent distribution and separated by bounding surfaces stacked in a zigzagging pattern, are consistent with the architecture expected for a sinuous linear dune with a strong longitudinal behaviour (Rubin, 1987; Rubin et al., 2008; Rubin and Hunter, 1985). However, the dimensions of the set bodies indicate the presence of a larger bedform in comparison to the first complex. Regarding the wedge-shaped bodies, their paleocurrent directions, their intra-set body cross-bedding dip-azimuth variability, and the evidence of dominant wind-ripple activity, indicate that they represent relatively stable dune sectors with little sinuosity. Sectors with these characteristics are very common in large linear dunes (larger than *seifs*, with a width over 100 m), where they represent the majority of the bedform section down to the dune toe

(Lancaster, 1995), and are herein referred to as dune flanks. The trough-shaped sets on the other hand, are interpreted as the deposits of the more active and sinuous crest area, given their position in the section core, the aeolian stratification types present, the paleocurrent directions and the intra-set body cross-bedding dip-azimuth variability. Considering that the dip-azimuths of bounding surfaces within this complex are oblique to the paleocurrent directions of the set bodies they bound, and that such orientation depends on which flank is the surface located, such surfaces are interpreted as a product of along-crest migration of bedform sinuosity, either in the dune crest or flank sectors (Rubin, 1987; Rubin et al., 2008). The small sets at the top of the complex most likely represent the record of small, superimposed dunes, developed over large linear dune mentioned earlier. These sets are only preserved within concave upward surfaces, which suggest that superimposed bedforms were related to overall erosive sectors of their host bedform and had little potential to be incorporated into the bedform record.

Following this conceptual model, the architecture of Complex 2 is likely the result of a single, large linear dune evolving into a slipfaced linear *draa* as superimposed dunes developed, while sustaining a dominant longitudinal behaviour.

Complex 3

Description. Complex 3 is characterized by stacked, intermediate-scale, trough-shaped sets (maximum thickness between 1 and 5 m, mode of 2-3 m; apparent thickness between 5 and 40 m, mode 23 m, Table 2), better preserved in the southern flank (due to modern erosion of the outcrop, Fig. 6), that occupies a large area in the study section (52%). Soft-sediment deformation related to the subsequent transgression (Strömbäck et al., 2005) has locally modified the upper sectors of this complex, but not enough to prevent interpretations (Fig. 6). The paleocurrents from trough-shaped bodies of this complex show an acute bimodal distribution similar to the trough-shaped bodies of Complex 2 (Fig. 9). They are also characterized by wind-ripple lamination/grainflow couplets that pass abruptly into thin (one or two dm thick) wind-ripple abundant or dominated set body bases (Fig. 4B). Bounding surfaces within this complex are of concave upwards shape, given the trough shape of the sets they bound, and show a wide dip-azimuth distribution. These dip-azimuths span from 315° to 60° in the northern flank and 50° to 120° in the southern flank (Fig. 9), which can also be inferred from the apparent dip in the architectural panels (Fig. 6). The general dip-azimuth trend is therefore dependent, upon position within the section and therefore broadly similar to the bounding surface dip-azimuth trend of Complex 2. The upper surface that separates this complex from overlying marine reworking sandstone and evaporites facies, has been mapped in previous studies (Argüello Scotti and Veiga, 2015). Small-scale elongated features were apparent in the southern flank of the large-scale preserved bedform both from the surface reconstructions and from direct observation of the outcrops. These are oriented subparallel to the large-scale bedform and have a relief reaching up to 6m.

Interpretation. The trough-shaped bodies of intermediate scale represent, by their size and position within the section, the migration of superimposed dunes over the large-scale bedform. Therefore, the bounding surfaces within this complex are interpreted as superimposition surfaces. The large-scale bedform associated with this complex lacked an active slipface and its behaviour was controlled by the development of its superimposed dunes. By similarity in paleocurrent directions to the trough-shaped sets of the previous complex, it is inferred that the superimposed dune types at *draa* crest and upper flanks positions were of linear type and longitudinal behaviour. This is also indicated by the small-scale elongated features observed at the top of the complex, which represent the exceptional preservation of superimposed bedforms oriented subparallel to the large-scale preserved bedform. Other bedforms types, however, could have been present closer to the *draa* plinth. Some small-scale features with different orientation and morphometry (asymmetrical section, 2m relief and 100m wavelength) are present in the interdune area and clearly represent other bedform types (Argüello Scotti and Veiga, 2015).

Considering the characteristics of Complex 3, its deposition can be associated to the development of a slipfaceless linear *draa*, likely of compound type. The overall dip-azimuth distribution of the bounding surfaces, dependent upon position, indicates that superimposition of bedforms was preserved in both flanks of the host bedform. This indicates once again that the major bedform had an overall dominant longitudinal behaviour.

Perspectives gained from deterministic models

To gain further understanding of the bedform development conditions that could have led to the deposition of each complex, the program BEDFORMS (Rubin, 1987) was used. This software simulates bedforms by 3D surfaces from sine curves, and determines the sedimentary architecture resulting from the successive positions of such surfaces in time. Original models available for sinuous linear dunes were modified to test two different scenarios (Fig. 10): on a first model, the effect of bedform growth on sedimentary architecture was tested. The bedform represented has an along-crest sinuosity migration and a lateral component in bedform motion, the latter being and order of magnitude smaller than the former (considering rates observed in modern examples of Bristow et al., 2005; Rubin et al., 2008; Tsoar et al., 2004). The second model intends to represent the morphodynamics and resulting sedimentary architecture of a *seif* dune in detail. For that purpose, some of the most remarkable studies on the morphology (Bullard et al., 1995; Lancaster, 1995; Pye and Tsoar, 2009; Tsoar, 1982) and dynamics (Livingstone, 2003; Livingstone and Thomas, 1993; Rubin et al., 2008; Tsoar, 1986, 1983; Tsoar et al., 2004) of small sinuous linear dunes or *seifs* were consulted. The bedform represented has peaks and saddles with a spacing half to that of the wavelength of bedform sinuosity, and a high frequency cyclic variation in the symmetry of the dune section. As in the first model, a lateral migration component in dune migration is added. Lastly, it is important to highlight that both models have a climbing angle of 0°, to emulate non-accumulation conditions (*sensu* Kocurek, 1999) observed in the Troncoso Inferior Member at the study area.

The results from first bedform model show that with an important rate of bedform growth, sinuosity migration of a single dune can result in the deposition of a considerable number of cross-bedded set bodies. This is also apparent from the models developed by Bristow et al. (2000) and Rubin et al. (2008). Once the width of the bedform exceeds the sinuosity's amplitude, both flanks of the bedform are incorporated into its record. Moreover, as long as the width increment (growth) exceeds the rate of lateral migration, more set bodies will be incorporated into de record of both flanks of the dune with time. These results are key to explain the sedimentary architecture observed in the study section, especially for Complexes 1 and 2, highlighting that a single dune can give origin to a large number of set bodies separated by sinuosity migration surfaces.

The results from the second model show the expected effect of peaks and saddles on the angle formed between the bedform orientation and the two modes in cross-bedding dip directions observed in the set bodies (Fig. 10). This effect is independent from the lateral migration direction of the bedform. When comparing the orientation of the preserved *draa* and the two dominant modes in paleocurrent and bounding surface dip directions in its record, the southeast modes are far closer to the bedform orientation than the northern modes. This model therefore helps explain the asymmetry in this bimodal distribution.

Relative chronology of cross-bedded set bodies

To analyse the internal relative chronology of set bodies within architectural complexes, a relative superposition order was built from the architectural panels (in a similar fashion as Bristow et al., 2005; their Fig. 4). Because the complexity of the stacking, at an early stage the chronology is divided, and each flank of the study section (north flank and south flank) has an independent chronology. As a result, each set body is identified by a letter ("c" for centre, indicating the initial chronology, "n" for northern flank and "s" for southern flank) and a number (Fig. 6).

The resulting chronostratigraphic scheme (Fig. 11) confirms that the oldest sedimentary bodies lie at the section core and indicates the general tendency, already suggested by the complexes' architecture and further confirmed by complexes' distribution, that the record of the studied bedform was deposited from a core outward, forming what can be described as a concentric record. From Complex 1 into Complex 2, there is a noticeable asymmetry in this concentric distribution, being the northern flank the one with the most perceivable expansion in relation to the position of the dune core. On Complex 3 however, this asymmetry is reverted, being the southern flank the one that experienced the biggest expansion from the previous complex. The asymmetry in both complexes cannot be precisely quantified because of the discontinuous record in the northern flank.

Distribution of architectural complexes

The distribution of each architectural complex was analysed across a width-corrected study section, in order to better represent the actual dimensions in a transversal cut of the *draa*. Over this corrected section, the general distribution of the complexes was mapped from the sedimentary logs and from virtual logs in the architectural panel (Fig. 12), which allowed for determining areal percentage occupied by each complex, measuring their width and height, contrasting the abundance in each sector, and establishing superposition relationships between the complexes.

Complex 2 and 3 comprise almost the whole *draa* record, combining for 99% of the section area. These complexes share the record in similar parts (Fig. 12). While Complex 2 is more abundant in the section centre, Complex 3 is far more abundant towards the *draa* flanks. Each complex extends successively higher in the body of the preserved bedform and occupies a wider lateral section than the previous complex. Complex 1 has a corrected width of 50 m and around 2 m in height, Complex 2 has a corrected width of around 350 m and a height of approximately 20 m, and Complex 3 has a corrected width of 860 m with a preserved height of 24 m. As such, the distribution of the complexes could be vaguely described as concentric, and it is yet another evidence of the bedform record being constructed from a core outward.

At his point it is important to consider the distribution of marine reworking facies that overlie the study section, studied by Strömbäck et al. (2005) and mapped by Argüello Scotti and Veiga (2015). These facies are believed to have been formed by saturation and wave action during marine flooding, leading to collapse and remobilization of dune sand. They are nearly absent in the dune crest but are thickest in dune flanks and interdune areas. Therefore, it is interpreted that aeolian sand remobilization from the crest to the flank sectors has reduced preserved bedform height and the relative volumetric importance of Complex 3, which accounts for its low proportion in the crest sector.

Discussion

Conceptual development model of the studied draa

Data analysis from this study demonstrates that each complex has been formed by a particular phase in bedform development, in which a combination of a specific bedform behaviour, growth, and evolution results in a particular sedimentary architecture style. Each phase can be related to one or more bedform configurations. Overall, the deposits of the studied preserved bedform record a story of gradual development though the configurations of small *seif* dune (likely also from an incipient bedform), large linear dune, slipfaced linear *draa* and finally a slipfaceless linear *draa* (Fig. 13).

Analysis from Complex 1, indicates that the oldest registered phase of bedform development was characterized by the development of a small *seif* dune configuration from an incipient bedform, possibly a dome dune or the tip of a *seif* dune, within a deflationary context associated with the development of a sand drift surface (Fig. 13A).

Complex 2 represents the second phase in bedform development (Fig. 13B), likely triggered by the continuation of the drying-upwards trend. The initiation of this phase is related to the evolution of a large linear dune from the previous small *seif*. This large linear dune had well-developed flanks and plinths and a more sinuous and mobile crest. Gradual growth of this bedform eventually allowed for superimposed dunes to develop on its flanks, evolving as a result into a slipfaced linear *draa*. The change in the overall sedimentary architecture provoked by this evolution was minimal as superimposed set bodies make only 2% of the complex section area.

Complex 3 represents the third and final phase in bedform development, related to a slipfaceless linear *draa* configuration (Fig. 13C). This evolution results in a sedimentary architecture characterized by medium-scale set bodies, bounded by superimposition surfaces. Therefore, evolution to a slipfaceless *draa* (start of Phase 3) seems to provoke a relevant impact in the style of sedimentary architecture, in contrast to the initial change in dune configuration form large dune to a slipfaced *draa* (Phase 2).

The start and subsequent intensification of aeolian dune construction is most likely the continuation of a drying-upwards trend registered through the Lower Troncoso Member (Veiga et al., 2005). The oldest preserved deposits in Complex 1 still show some signs of deposition upon a damp accumulation surface, and, as drier conditions prevailed, gradually more sand might have become available triggering previously protracted aeolian dune construction. Therefore, sand availability might be the conditioning factor behind bedform evolution into large-size configurations.

This model is similar in many ways to the model of bedform development presented by Bristow et al. (2000) built from several GPR transects in along the tip of a large linear dune/*draa*. However, in the example provided by the present study, the sedimentary architecture related to the simple dune configuration is far more complex, formed by a large number of cross-bedded set bodies. This difference is most likely related to a longer-lived linear dune configuration in the Troncoso example, along with consistent gradual bedform growth and a more dominant longitudinal behaviour.

Conditioning factors over the development of the studied bedform

The internal characteristics of the architectural complexes and their distribution (Figs. 6, 9, 11, 12) indicate that the preserved bedform had an overall consistent and dominant longitudinal behaviour throughout its recorded development. This does not prove that the bedform did not undergo lateral migration; in fact, the construction and distribution of each complex has a certain degree of asymmetry that indicates a lateral component. However, through all the complexes, evidence indicates that the bedform produced deposition on both flanks, even under the effect of lateral migration. Considering that this bedform never produced accumulation (*sensu* Kocurek, 1999), then the process that allows both flanks to be preserved must be bedform growth (i.e. increment in bedform scale) and not accretion (i.e. rise in the accumulation surface).

Therefore, during the development of this bedform, lateral migration rates were surpassed by a growth component. Even if growth in one flank is favoured in relation to the other, both flanks showed an overall long-term growth. From all of the above, bedform growth together with a dominant longitudinal behaviour were the crucial factors in shaping the sedimentary architecture of the preserved bedform.

It is likely that after the bedform had stopped its growth as a *draa*, a little component of lateral migration could have completely changed its sedimentary architecture given sufficient time. However, such lateral migration rate should have been consistent and sustained through the extended periods of time that these bedforms need to reach equilibrium with environmental conditions (which are rarely achieved). In this case, marine transgression of the Troncoso Sand Sea hindered further development of this bedform.

Since the genetic link between different types of linear aeolian bedforms has been mostly inferred, and rarely documented (Warren, 2013), the record of the studied preserved *draa* provides an exceptional example of the evolution between different type of aeolian linear bedforms during the development of a large linear *draa*. It documents the link between small *seif* dunes, large linear dunes and linear *draa*, and in particular, the scale at which the transition between a simple dune and a *draa* occurs, that is as the bedform width reaches 300-400 m. The particular growth dominated-development of the studied bedform seems to be the main reason behind the preservation of bedform evolution.

Sinuosity migration surfaces: a bounding surface type for simple linear dunes

Detailed analysis of the architecture of Complex 1 and 2, together with the lessons learned from deterministic models and previous studies of linear dune architecture and behaviour (Bristow et al., 2000; Rubin, 1987; Rubin et al., 2008; Tsoar, 1983), highlight that the internal architecture of simple sinuous linear dunes is characterized by the predominance of large-scale bounding surfaces generated by the longitudinal (along-crest) migration of the bedform sinuosity. The term “*sinuosity migration surfaces”* is suggested in this study to refer to such bounding surface type.

The particular characteristics of this bounding surface type are dip-azimuths which are oblique to the paleocurrent directions of the set bodies they bound and strikes subparallel to the bedform orientation. If both flanks of the bedform are preserved in the rock record, then two modes of surface dip-azimuths will be recorded. The angle between these two modes will likely be a high obtuse angle and each dip-azimuth mode will be dominant in the respective flank of the bedform record. If, on the other hand, only one flank of the dune is preserved due to a predominance of lateral migration, the dip-azimuth distribution of the preserved surfaces will have only one clear mode. In the context of autocyclic surfaces generated by aeolian bedforms, the hierarchy of sinuosity migration surfaces is lower than that of interdune migration and superimposition surfaces, and higher to that of reactivation surfaces. This surface type introduces a remarkable complexity into the deposits of a simple dune, and its impact upon identification and sedimentary heterogeneity characterization in this type of deposits must be highlighted.

Estimating bedform orientation from the strike of this bounding surface, although a much more accurate indicator than paleocurrent orientation, must be exercised with caution.

As the two modes of dip-azimuths are not bipolar, one must choose between one of the modes, or perform the bisector between the two. In this regard, more theoretical and field work is needed to determine the causes that lead to a non-bipolar dip-azimuth distribution.

Factors conditioning the sedimentary architecture of linear bedforms

As with any other bedform type, behaviour, growth, and evolution are major factors that condition the resulting sedimentary architecture of aeolian linear bedforms (alongside for example, the relative motion of the accumulation surface). However, some of the discussed factors gain or lose relative importance for this particular bedform type.

What this case study in particular suggests, is that bedform growth can be an important conditioning factor in the long-term development linear bedforms and particularly critical in shaping its internal sedimentary architecture. Growth exponentially reduces the lateral migration rate of a linear bedform by reducing its surface/volume relationship. Furthermore, as growth doesn't potentially impact along-crest sand transport, it should favour a longitudinal bedform behaviour. In other words, growth has a considerable impact in behaviour. This likely indicates that as linear bedforms reach large dune and especially *draa*-scale sizes, lateral migration rates became so low that its influence over the preserved internal architecture could be greatly overshadowed by other factors. The far more mobile transverse ridges (*sensu* Rubin and Hunter, 1985) provide an opposite extreme in relative importance of conditioning factors. In transverse bedforms, any effect of a growth component will not produce a lasting impact in the sedimentary architecture, due to the far larger migration rates of these bedforms. The overall sedimentary architecture in that case will be more influenced by bedform scale and behaviour along with relative motion of the accumulation surface.

Finally, it must also be considered that the parameters associated to bedform development are ultimately controlled by the larger dunefield self-organization, which dictates the bedform pattern of the system (Kocurek and Ewing, 2005). This can explain why the record of adjacent linear bedforms (or even the record of the same bedform along its extension) can be quite different, as seen in the many dunes studied in the northern extreme of the Namib Sand Sea (Bristow et al., 2007, 2005, 2000).

Models of linear bedform sedimentary architecture

Considering previous case studies and the example provided in this study, assigning a simple model of the expected sedimentary architecture for sandy, aeolian linear bedforms is far from a simple task. The overall internal architecture of aeolian linear bedforms however, can be considered to vary from two opposite endmembers (Fig. 14): a concentric style, where the oldest deposits are found in the bedform core (e.g. bedform studied in this paper), and an asymmetric style, where the oldest deposits are found in one of the flank's extremes (e.g. Warsaw Dune studied by Bristow et al. (2005). This differentiation can be made for the deposits of both simple and compound/complex bedforms. Bounding surface's dip-azimuths would be bimodal and dependent upon their position in the concentric style, while they would be unimodal and evenly distributed in the asymmetric counterpart. In the concentric style, the architecture will likely be conditioned by growth and/or accretion, along with a strong sustained longitudinal behaviour. If the style of architecture is on the other hand asymmetric, the architecture is likely to have been strongly conditioned by a sustained and consistent lateral migration. This scheme departs from earlier classifications (Fig. 1) by using a descriptive terminology, independent from the possible mechanisms that may have shaped the sedimentary architecture and from the simple/compound/complex nature of the originating bedform.

Previous studies that have encountered a sedimentary architecture resembling a concentric style, have attributed it to accretion of the bedform pattern (Bose et al., 1999; Rubin and Hunter, 1985). However, Rubin and Hunter (1985) made it clear that the natural conditions necessary for accretion of a bedform pattern of linear dunes that would allow preservation of both flanks in the geological record (with a climbing angle of at least 30°), are very specific and would be extremely uncommon and restricted spatially. Therefore, considering the slow migration rates for these bedforms, sustained bedform growth can be a development scenario far more likely than accretion to account for the preservation of this style of sedimentary architecture. If the notion, under aeolian sequence stratigraphic conceptual framework (Kocurek, 1999), that accumulation is not necessary for preservation is also considered (a common scenario for ancient deposits of linear bedforms; e.g. Entrada Sandstone, Lower Permian Yellow Sands, Botucatu Formation, Troncoso Inferior Member), then the conditions necessary for a linear dune to preserve a more “classic” sedimentary architecture style of bimodal cross-bedding and bounding surface dip directions may not be unusual in cases of preserved bedform morphology.

Conclusions

The methodology followed in this paper was successful in identifying significant qualitative and quantitative differences within the sedimentary architecture exposed in a natural section of a preserved linear bedform belonging to the ancient Troncoso Sand Sea. These differences allowed for the identification of three different sedimentary architecture styles or architectural complexes. These were demonstrated to be formed by genetically-related cross-bedded set bodies and bounding surfaces, associated to a specific phase in bedform development in which bedform evolution, behaviour and growth resulted in a relatively homogeneous style of sedimentary architecture.

A conceptual model for the development of the studied preserved bedform was presented, composed by three phases. Phase one comprises a possible incipient bedform (dome dune or *seif* dune tip) evolving into a small linear *seif*. Phase two represents the development of a large linear dune that evolves into a slipfaced linear *draa*. Finally, phase three is characterized by a slipfaceless linear *draa* coincident to the final preserved morphology of the bedform.

Development of the studied preserved bedform was characterized by sustained growth and a dominant longitudinal behaviour, which were the key parameters shaping its final internal architecture, while the lateral migration component in bedform behaviour was never a critical factor. Preservation of bedform evolution provided a unique example to document the link between different types of linear bedforms.

Characterization of the preserved bedform's record allowed for discussing which parameters are most critical in shaping the sedimentary architecture of linear bedforms. It suggests that growth can be an important factor for this bedform type given their low migration rates, which became exponentially lower as the bedforms increase their size.

Finally, linear bedform deposits can be characterized by two contrasting styles of sedimentary architecture: a concentric style, and an asymmetric style. In the former, the oldest deposits are found in the bedform core, while on the latter, the oldest deposits are found in one of the flank's extremes. The characteristics of the bounding surfaces in each case were analysed, and the likely controlling factors behind each style of architecture were determined. As a concentric architecture generated by accretion requires conditions regarded as very unlikely in nature, consistent bedform growth and dominant longitudinal behaviour can be considered as a likely scenario to account for this architecture type and suggests that its occurrence may not be unusual in the geological record.

References

Aguirre-Urreta, B., Schmitz, M., Lescano, M., Tunik, M., Rawson, P.F., Concheyro, A., Buhler, M., and **Ramos, V.A.** (2017) A high precision U–Pb radioisotopic age for the Agrio Formation, Neuquén Basin, Argentina: Implications for the chronology of the Hauterivian Stage. *Cretaceous Res.*, **75**, 193-204.

Ahmed Benan, C.A. and **Kocurek, G.** (2000) Catastrophic flooding of an aeolian dune field: Jurassic Entrada and Todilto formations, Ghost Ranch, New Mexico, USA. *Sedimentology*, **47**, 1069-1080.

Argüello Scotti, A. (2017) Origen, arquitectura interna y evolución secuencial del Sistema Eólico Barremiano en el centro-este de la Cuenca Neuquina: modelado tridimensional e implicancias para la caracterización de reservorios de origen eólico (*Doctoral Thesis*). Universidad Nacional de La Plata, La Plata, 235 pp.

Argüello Scotti, A. and **Veiga, G.D.** (2015) Morphological Characterization of an Exceptionally Preserved Eolian System: the Cretaceous Troncoso Inferior Member in the Neuquén Basin (Argentina). *Latin Am. J. Sedimentol. Basin Anal.*, **22**, 29-46.

Bagnold, R.A. (1941) The Physics of Blown Sand and Desert Dunes. Methuen & Company, London, 265 pp.

Bose, P.K., Chakrabarty, S. and **Sarkar, S.** (1999) Recognition of ancient eolian longitudinal dunes; a case study in upper Bhander Sandstone, Son Valley, India. *J. Sed. Res.*, **69**, 74-83.

Bristow, C.S., Bailey, S.D. and **Lancaster, N.** (2000) The sedimentary structure of linear sand dunes. *Nature*, **406**, 56-59.

Bristow, C.S., Duller, G.A.T. and **Lancaster, N.** (2007) Age and dynamics of linear dunes in the Namib Desert. *Geology*, **35**, 555-558.

Bristow, C.S., Lancaster, N. and **Duller, G.A.T.** (2005) Combining ground penetrating radar surveys and optical dating to determine dune migration in Namibia. *J. Geol. Soc. London*, **162**, 315-321.

Bullard, J.E., Thomas, D.S.G., Livingstone, I. and **Wiggs, G.F.S.** (1995) Analysis of linear sand dune morphological variability, southwestem Kalahari Desert. *Geomorphology*, **11**, 189-203.

Cignoni, P., Corsini, M. and **Ranzuglia, G.** (2008) MeshLab: an open-source 3D mesh processing system. *ERCIM News*, **73**, 45-46.

Clemmensen, L.B. (1989) Preservation of interdraa and plinth deposits by the lateral migration of large linear draas (Lower Permian Yellow Sands, northeast England). *Sed. Geol.*, **65**, 139-151.

Clemmensen, L.B. and **Tirsgaard, H.** (1990) Sand-drift surfaces: a neglected type of bounding surface. *Geology*, **18**, 1142-1145.

Collinson, J.D., Mountney, N.P. and **Thompson, D.B.** (2006) Sedimentary Structures. Terra, Harpenden, 292 pp.

Dajczgewand, D., Nocioni, A., Fantin, M., Minniti, S., Calegari, R. and **Gavarrino, A.** (2006) Lower Troncoso eolian bodies identification in the Neuquen Basin, Argentina: a different approach and some geological implications. *Extended abstract from the 9th Simposio Bolivariano - Exploración Petrolera en las Cuencas Subandinas*, Cartagena, Colombia.

Glennie, K.W. (1972) Permian Rotliegendes of Northwest Europe interpreted in light of modern desert sedimentation studies. *AAPG Bull.*, **56**, 1048-1071.

Groeber, P. (1946) Observaciones geológicas a lo largo del meridiano 70. Hoja Chos Malal. *Revista de la Sociedad Geológica Argentina,* **1**, 177-208.

Havholm, K., Kocurek, G. (1994) Factors controlling aeolian sequence stratigraphy: clues from super bounding surface features in the Middle Jurassic Page Sandstone. *Sedimentology*, **41**, 913-934.

Howell, J.A., Schwarz, E., Spalletti, L.A. and **Veiga, G.D.** (2005) The Neuquén Basin: an overview. In: *The Neuquén Basin, Argentina: A Case Study in Sequence Stratigraphy and Basin Dynamics* (Eds G.D. Veiga, L.A. Spalletti, J.A. Howell and E. Schwarz), *Geol. Soc. London Spec. Publ.*, 252, 1-14.

Hunter, R.E. (1977) Basic types of stratification in small eolian dunes. *Sedimentology*, **24**, 361-387.

Kocurek, G. (1999) The aeolian rock record (Yes, Virgina, it exists, but it really is rather special to create one). In: *Aeolian Environments Sediments and Landforms* (Eds A.S. Goudie, I. Livingstone and S. Stokes), pp. 239-259. John Wiley and Sons, Chichester.

Kocurek, G. and **Dott, R.H.** (1981) Distinctions and Uses of Stratification Types in the Interpretation of Eolian Sand. *J. Sed. Res.*, **51**, 579-595.

Kocurek, G. and **Ewing, R.C.** (2005) Aeolian dune field self-organization - Implications for the formation of simple versus complex dune-field patterns. *Geomorphology*, **72**, 94-

105.

Kocurek, G., Knight, J. and **Havholm, K.** (1991) Outcrop and semi-regional three-dimensional architecture and reconstruction of a portion of the eolian Page Sandstone (Jurassic). In: *The Three-Dimensional Facies Architecture of Terrigenous Clastic Sedi-Ments and Its Implications for Hydrocarbon Discovery and Recovery* (Eds A.D. Miall and N. Tyler), *SEPM Spec. Publ.*, **3**, 25-43.

Lancaster, N. (1995) Geomorphology of Desert Dunes. Routledge, London, 290 pp.

Lancaster, N. (1982) Linear dunes. *Prog. Phys. Geogr.*, **6**, 475-504.

Lazo, D.G. and **Damborenea, S.E.** (2011) Barremian bivalves from the Huitrín Formation, west-central Argentina: taxonomy and paleoecology of a restricted marine association. *J. Paleontol.*, **85**, 719-743.

Livingstone, I. (2003) A twenty-one-year record of surface change on a Namib linear dune. *Earth Surf. Proc. Land.*, **28**, 1025-1031.

Livingstone, I. and **Thomas, D.S.G.** (1993) Modes of linear dune activity and their palaeoenvironmental significance: an evaluation with reference to southern African examples. In: *The Dynamics and Environmental Context of Aeolian Sedimentary Systems* (Ed. K. Pye),. *Geol. Soc. London Spec. Publ.*, 72, 91-101.

Livingstone, I. and **Warren, A.** (1996) Aeolian Geomorphology: an Introduction. Longman, Essex, 221 pp.

McKee, E.D. (1983) Eolian Sand Bodies of the World. *Dev. Sedimentol.*, **38**, 1-25.

McKee, E.D. and **Tibbitts, G.C.** (1964) Primary Structures of a Seif Dune and associated deposits in Libya. *J. Sed. Petrol.*, **34**, 5–17.

Mountney, N.P. (2006) Eolian Facies Models. In: *Facies Models Revisited* (Eds H.W. Posamentier and R.G. Walker), *SEPM Spec. Publ.*, **84**. 19-83.

Pye, K. and **Tsoar, H.** (2009) Aeolian Sand and Sand Dunes. Springer, Berlin, 458 pp.

Rubin, D.M. (1987) Cross-Bedding, Bedforms, and Paleocurrents. *Concepts in Sedimentology and Paleontology*, **1**, 187 pp.

Rubin, D.M. and **Hunter, R.E.** (1985) Why deposits of longitudinal dunes are rarely recognized in the geologic record. *Sedimentology*, **32**, 147-157.

Rubin, D.M., Tsoar, H., and **Blumberg, D.G.** (2008) A second look at western Sinai seif dunes and their lateral migration. *Geomorphology*, **93**, 335-342.

Scherer, C.M.S. (2000) Eolian dunes of the Botucatu Formation (Cretaceous) in southernmost Brazil: Morphology and origin. *Sed. Geol.*, **137**, 63-84.

Steele, R.P. (1983) Longitudinal Draa in The Permian Yellow Sands of North-East England. *Dev. Sedimentol.*, **38**, 543-550.

Strömbäck, A., Howell, J.A. and **Veiga, G.D.** (2005) The transgression of an erg - sedimentation and reworking/soft-sediment deformation of aeolian facies: the Cretaceous Troncoso Member, Neuquén Basin, Argentina. In: *The Neuquén Basin, Argentina: A Case Study in Sequence Stratigraphy and Basin Dynamics* (Eds G.D. Veiga, L.A. Spalletti, J.A. Howell and E. Schwarz), *Geol. Soc. London Spec. Publ.*, 252, 163-183.

Tsoar, H. (1989) Linear dunes - forms and formation. *Prog. Phys. Geogr.*, **13**, 507-528.

Tsoar, H. (1986) The advance mechanism of Longitudinal Dunes. In: *Physics of Desertification* (f. El-Baz and H. Mohammed) pp. 241-250. Martinus Nijhoff, Dordrecht.

Tsoar, H. (1983) Dynamic processes acting on a longitudinal (seif) sand dune. *Sedimentology*, **30**, 567-578.

Tsoar, H. (1982) Internal structure and surface geometry of longitudinal (seif) dunes. *J. Sed. Res.*, **52**, 823-831.

Tsoar, H., Blumberg, D.G. and **Stoler, Y.** (2004) Elongation and migration of sand dunes. *Geomorphology*, **57**, 293-302.

Veiga, G.D., Howell, J.A. and **Strömbäck, A.** (2005) Anatomy of a mixed marine-non-marine lowstand wedge in a ramp setting. The Record of a Barremian-Aptian complex relative sea-level fall in the central Neuquen Basin, Argentina. In: *The Neuquén Basin, Argentina: A Case Study in Sequence Stratigraphy and Basin Dynamics* (Eds G.D. Veiga, L.A. Spalletti, J.A. Howell and E. Schwarz), *Geol. Soc. London Spec. Publ.*, 252, 139-162.

Warren, A. (2013) Dunes: Dynamics, Morphology, History. Wiley-Blackwell, Chichester, 236 pp.

Wilson, I.G. (1972) Aeolian bedforms-their development and origins. *Sedimentology*, **19**, 173-210.

Wu, C. (2011) VisualSFM: A Visual Structure from Motion System. *Retrieved from http://ccwu.me/vsfm/*.

Table Captions

Table 1. Terminology used in this study. Major bedform parameters, at a certain time and their variability over a particular time period, that determine sedimentary architecture in the geological record.

Table 2. Differences in scale and geometry between cross-bedded set body populations of different architectural complexes

Table 3. Results of applying Tuckey's and Dunn's multiple comparisons tests for maximum thickness and apparent width for cross-bedded set body populations of different architectural complexes.

Table 4. Summary of the differences between wedge- and trough-shaped set bodies found in Complex 2.

Figure Captions

Figure 1. Models of linear bedform sedimentary architecture, their dominant characteristics, inferred origin, and ancient examples. Both *draa* and simple dune references are taken into account. L.P.Y.S. stands for Lower Permian Yellow Sands.

Figure 2. Location of the Neuquén Basin, extension of the Troncoso Inferior Member and the Troncoso Sand Sea, and location of the study area.

Figure 3. Study area and section, and previous morphology studies in the locality. A) View of the Troncoso Inferior section in the study area, seen from the North. B) Map of the Troncoso Inferior Member outcrops and provincial roads around the study area, showing the location of the study section and the extension mapped in Argüello Scotti and Veiga (2015). C) Thickness map of the study interval in the study area, revealing the location, dimensions and orientation of the large-scale preserved bedforms. D) Study interval's thickness variation in

the study section, flattened at the base, showing external geometry features of the preserved bedform, which are further used as reference for the position of internal sedimentary bodies and surfaces.

Figure 4. Sedimentary facies and stratification types typical of the study interval. A) Large-scale cross-bedded sandstones passing abruptly downwards into subhorizontal laminated sandstones. B) Clearly recognizable individual high-angle grainflow strata wedging out into low-angle wind-ripple lamination (climbing translatent strata) in the bottom of a cross-bedded set body. C) Grainflow strata separated by thin grainfall laminae (marked by black arrows). D) Close up of a wind-ripple lamination dominated sector of a cross-bedded set body.

Figure 5. Workflow used to characterize and analyse the sedimentary architecture of the study section. Data acquisition and analysis are separated as the main stages of the workflow. Concrete tasks are shown in italics, acquisition results are shown in white boxes, specific elements of study are shown in grey boxes, and analysis are shown in regular text.

Figure 6. Sedimentary architecture of the studied section. A) Close up of the photomosaic shown in Fig. 2A, with the study section marked in yellow. B) Architectural panel a-a' (location on Figs. 2B, 6A). C) Architectural panel b-b' (Location on Fig. 2B). D) Architectural panel c-c' (Location on Fig. 2B). All panels show identified architectural complexes (see text for further details), discerned by colour, and cross-bedded set body identifications tags.

Figure 7. Histograms indicative of cross-bedded set body scale, discriminated by architectural complex. A) Frequency of set body's maximum thickness. B) Frequency of set body's apparent width.

Figure 8. Details of set bodies and bounding surfaces belonging to different complexes. A) Small-scale set bodies from Complex 1, showing a stacking that forms a zigzagging arrangement of the intervening bounding surfaces (pen for scale). B) Detail of a climbing adhesion ripple stratum (lower limit marked by white arrow) found at the top of the C1 set body. Climbing translatent strata dip to the left and therefore climb in the opposite direction. C) Thin section of a sample taken from Complex 1 (location on Fig. 6B) showing the abundance of clasts of opaque minerals. D) Large-scale trough-shaped set body from

Complex 2. Towards the top of the picture, very small-scale set bodies also from Complex 2 are grouped within a concave upwards bounding surface. E) Interval dominated by wind-ripple lamination, highlighted by reddish colour, between massive-looking amalgamated grainflow intervals. This is referred to as wind-ripple/grainflow couplets in the text, which are the most common form of aeolian stratification type distribution in the study section (repeated in Figs 8D, 8F). D) Large-scale wedge-shaped set bodies (n18-n19) from Complex 2. G) Wind-ripple lamination dominated lower sector of a wedge-shaped set body from Complex 2.

Figure 9. Paleocurrent (averaged cross-bedding values for each set body) and bounding surface dip-azimuth distribution, arranged by complex. Panel a-a' is shown as well, indicating not only the different architectural complexes but also the different set body types within Complex 2. Paleocurrents of Complex 2 are arranged by large-scale and very-small scale set bodies, and the former between trough-shaped and wedge-shaped sets. Bounding surfaces of Complex 2 are arranged by shape and position within the section.

Figure 10. Deterministic models generated in BEDFORMS. Model 1 shows the resulting architecture from bedform development characterized by growth. Model 2 shows the asymmetry in paleocurrent bimodal distribution in relation to the bedform trend, and the range of surface types expected in simple linear dunes. The higher-hierarchy surfaces bound cross-bedded set bodies and are formed by along-crest sinuosity migration. The lower-hierarchy surfaces are found within cross-bedded set bodies and are the result of dune profile cyclic variation.

Figure 11. Chronostratigraphic scheme based on architectural panel a-a'. The cross-bedded set bodies are ordered in time according to a possible order or relative superposition. The set bodies have upper erosive unconformable surfaces, indicated by cross-bedding truncation, and lower depositional conformable surfaces, indicated by cross-bedding downlap and therefore time transgressive. Interpreted phases of bedform development and their associated bedform configurations are shown in time. Note the fragmentary nature of

the bedform record and the gradual expansion of the preserved set bodies from a core outward.

Figure 12. Architectural complex distribution, geometry and dimensions, within the preserved *draa* record. Position of sedimentary logs used for control are shown as well. Preserved bedform and complex dimensions are calculated for what would be expected in a transversal section of the *draa*.

Figure 13. Conceptual model for development of the preserved *draa*. The diagrams show the phases of bedform development, inferred to be responsible for the deposition of the architectural complexes, and their associated bedform configurations.

Figure 14. Scheme showing the two inferred endmembers to which linear bedform sedimentary architecture can be related, their main characteristics, and inferred factors that may condition their development. The scheme is applicable to both simple a compound/complex linear bedforms.

Figure 1
Argüello Scotti and Veiga
(full width - 170 mm x 144 mm)

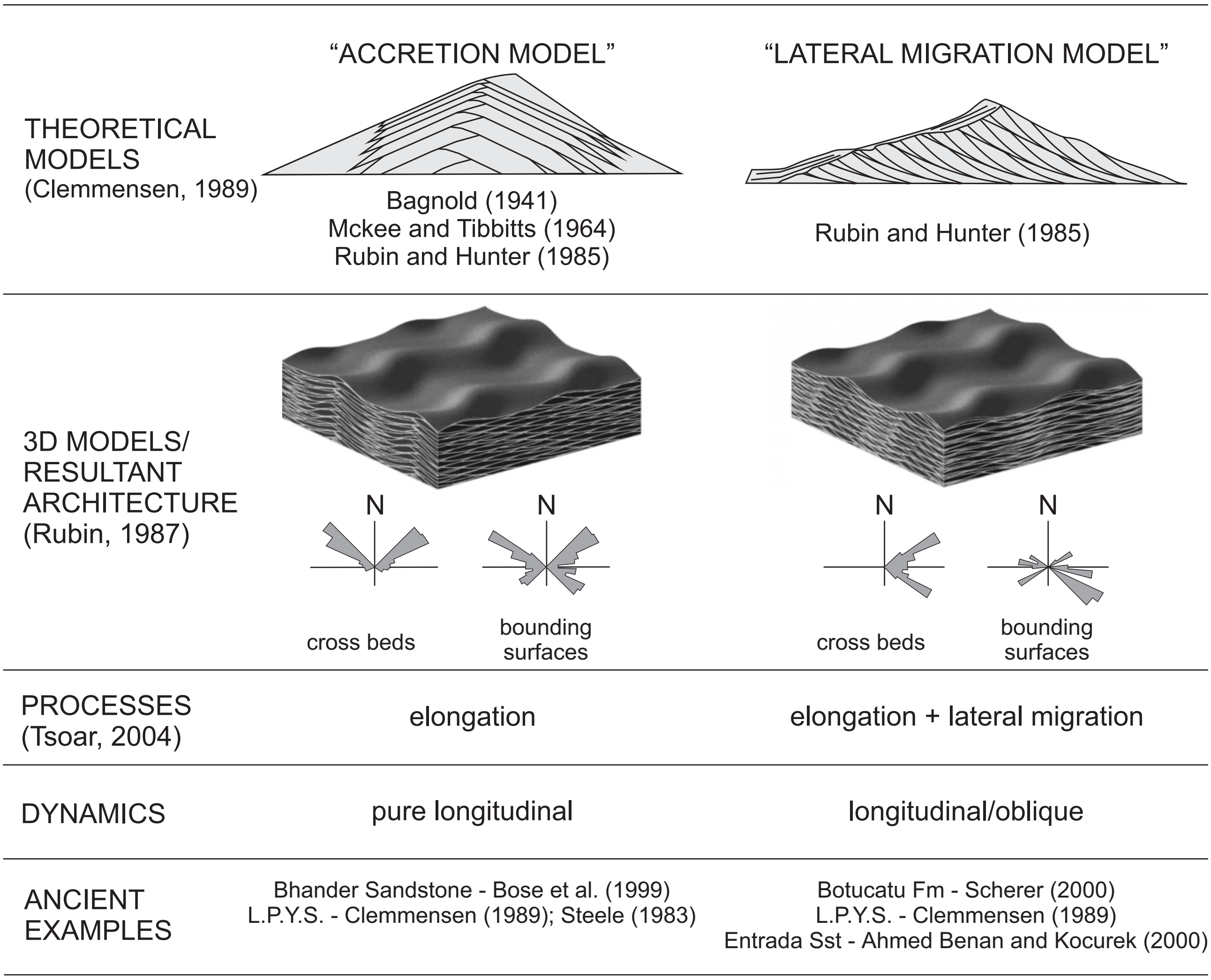

Figure 2
Argüello Scotti and Veiga
(column width - 80 x 86 mm)

Figure 3
Argüello Scotti and Veiga
(full width - 170 mm x 149 mm)

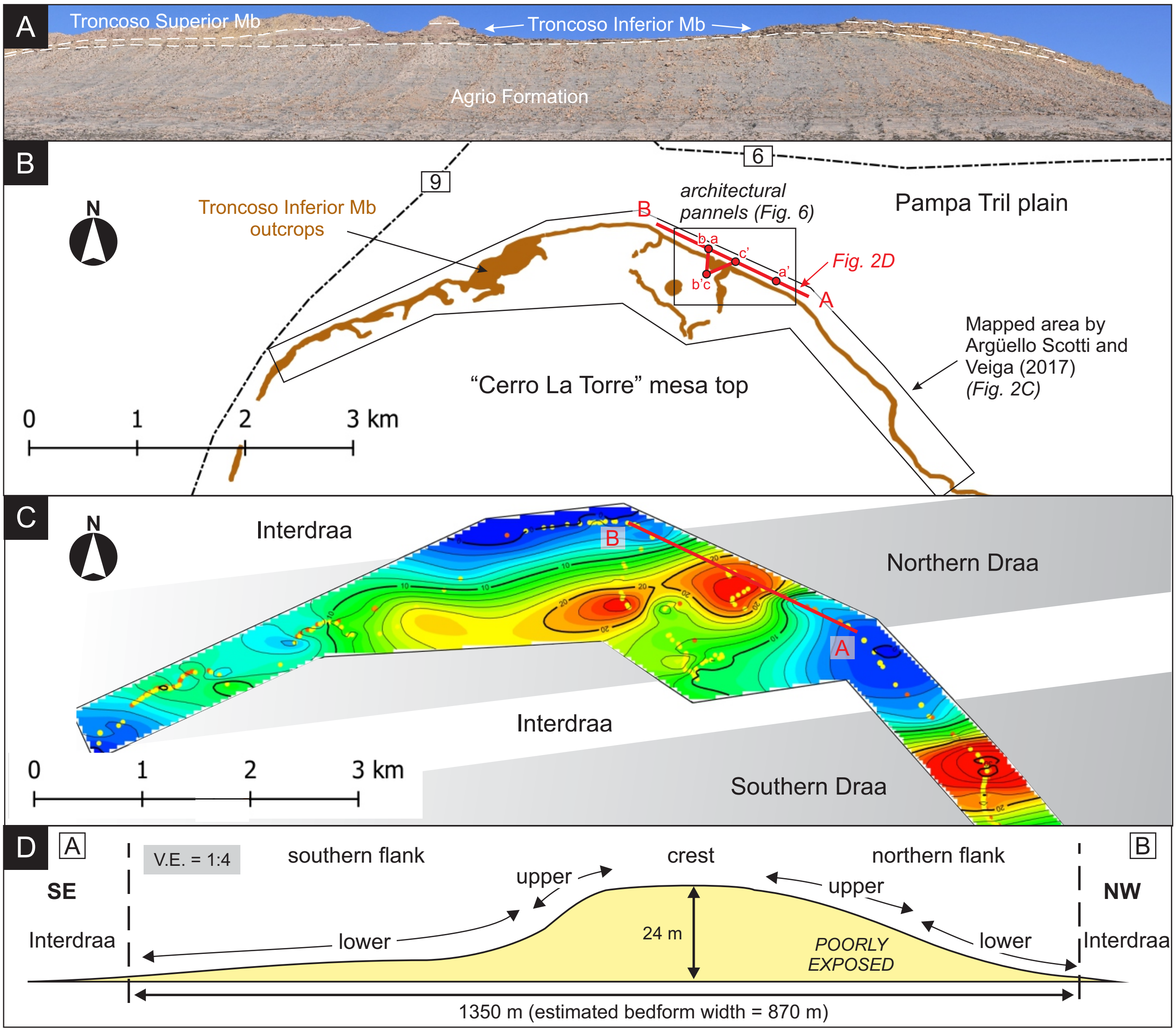

Figure 4
Argüello Scotti and Veiga
(full width - 170 mm x 170 mm)

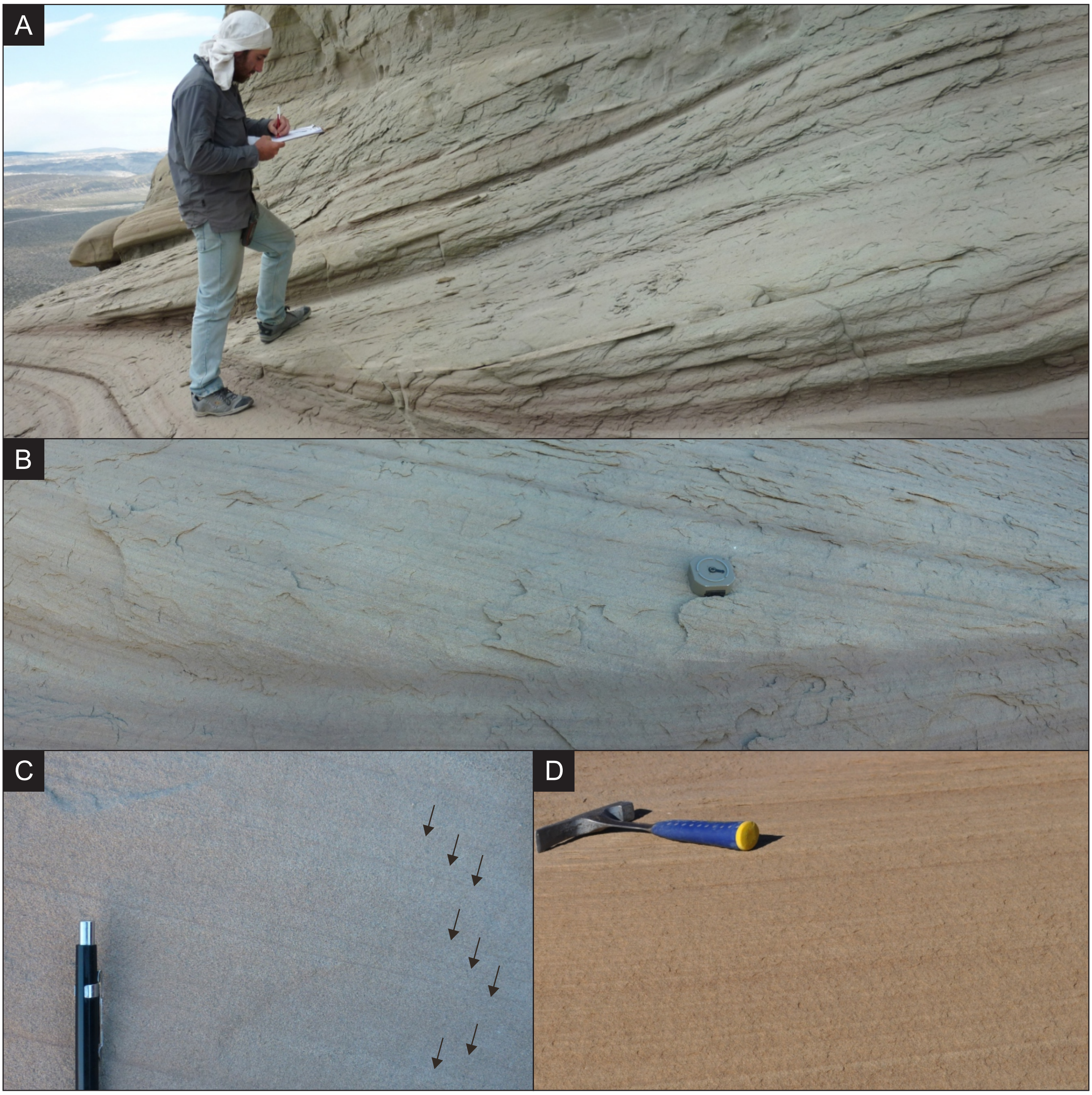

Figure 5
Argüello Scotti and Veiga
(full width - 170 mm x 111 mm)

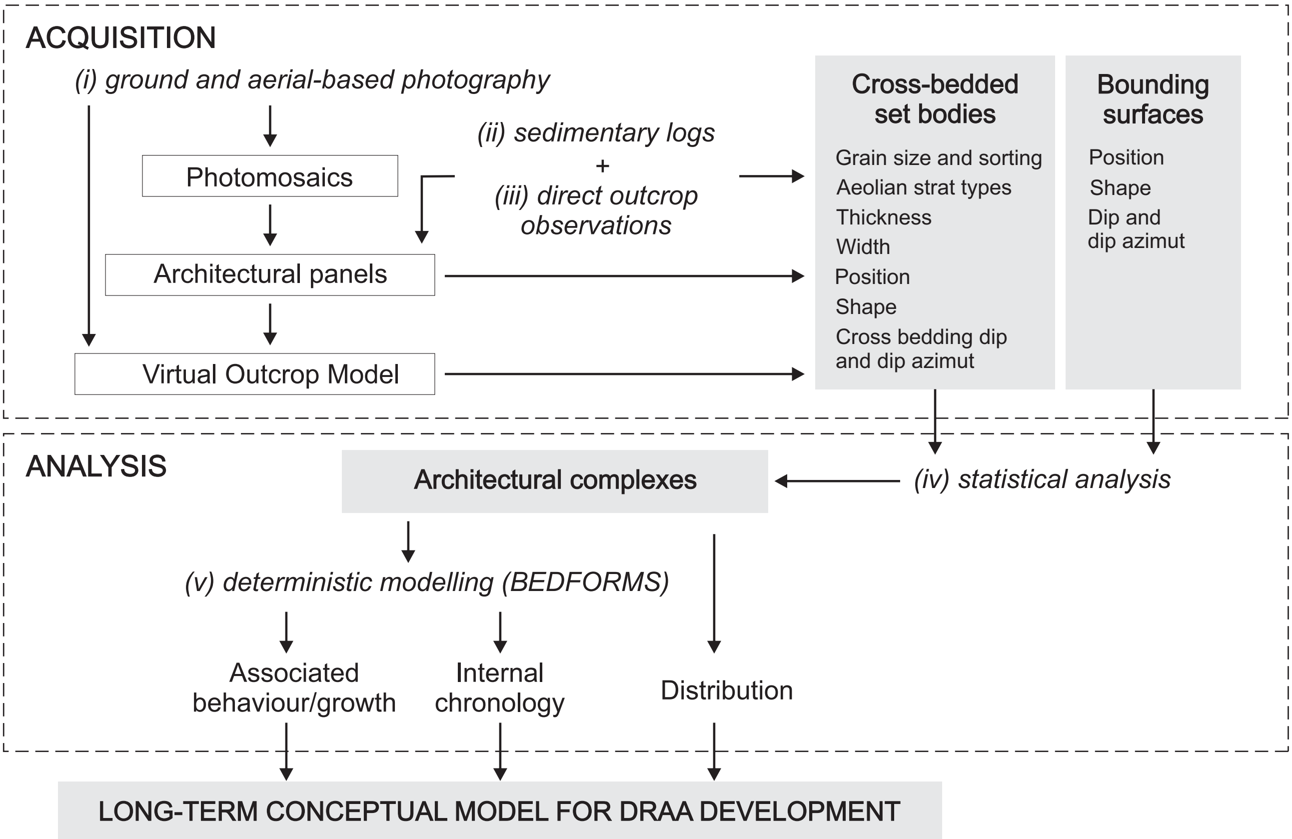

Figure 6
Argüello Scotti and Veiga
(fold out - full width landscape orientation 230 mm)

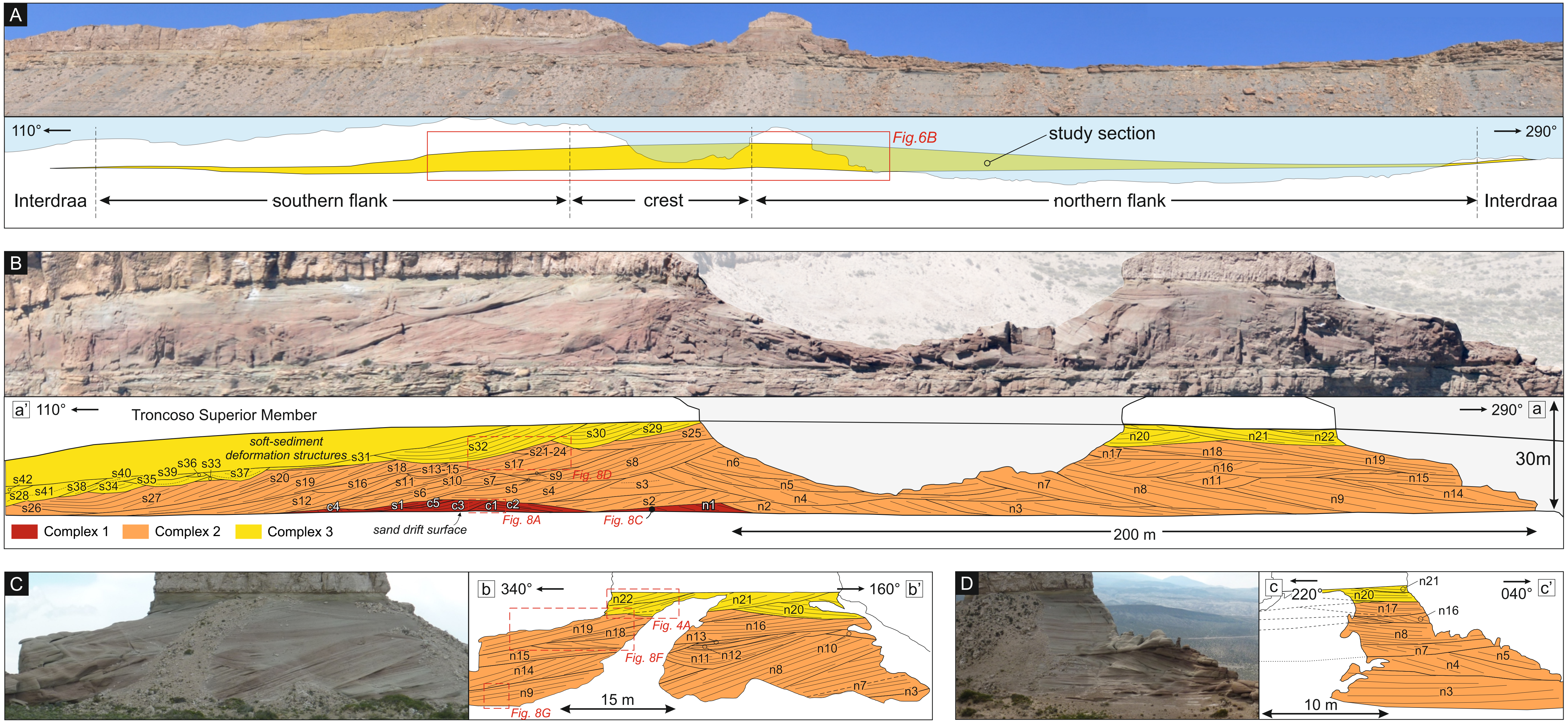

Figure 7
Argüello Scotti and Veiga
(2/3 page or 1 column)

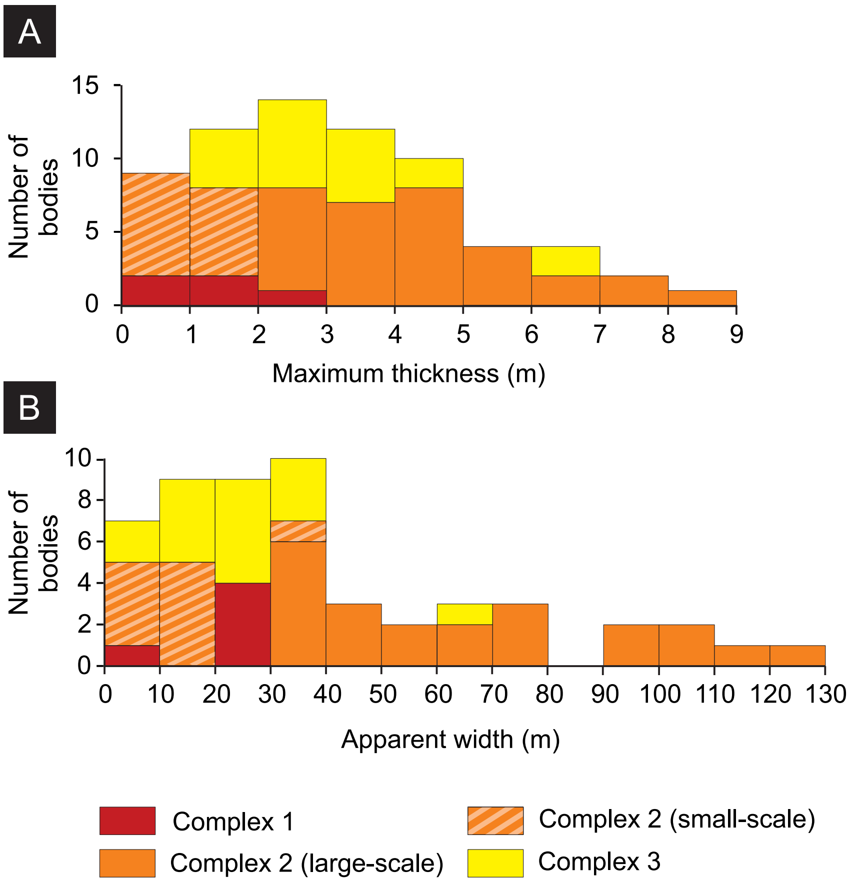

Figure 8
Argüello Scotti and Veiga
(full width - 170 mm x 178 mm)

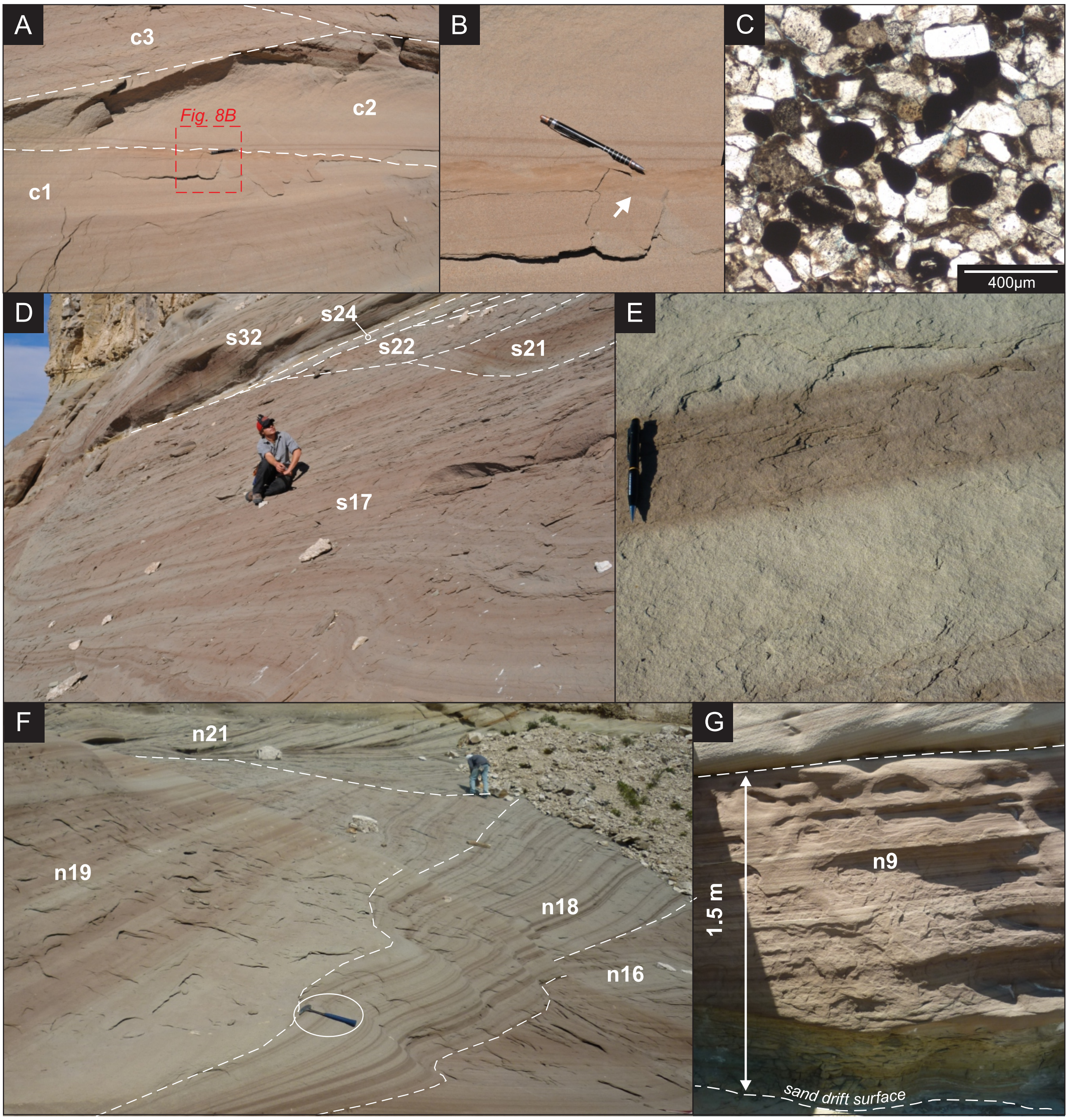

Figure 9
Argüello Scotti and Veiga
(170 mm x 110 mm)

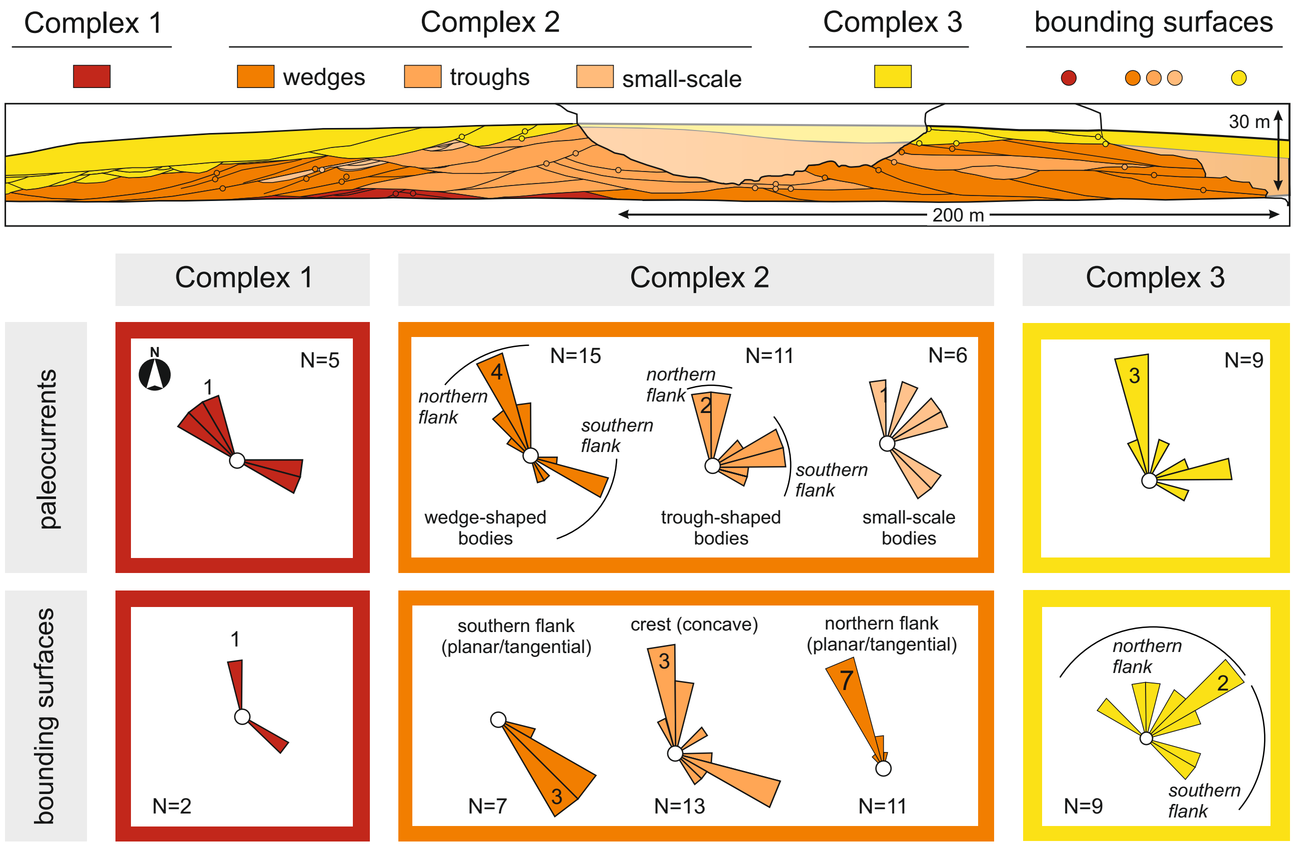

Figure 10
Argüello Scotti and Veiga
(2/3 page - 112 mm x 142 mm or full page width)

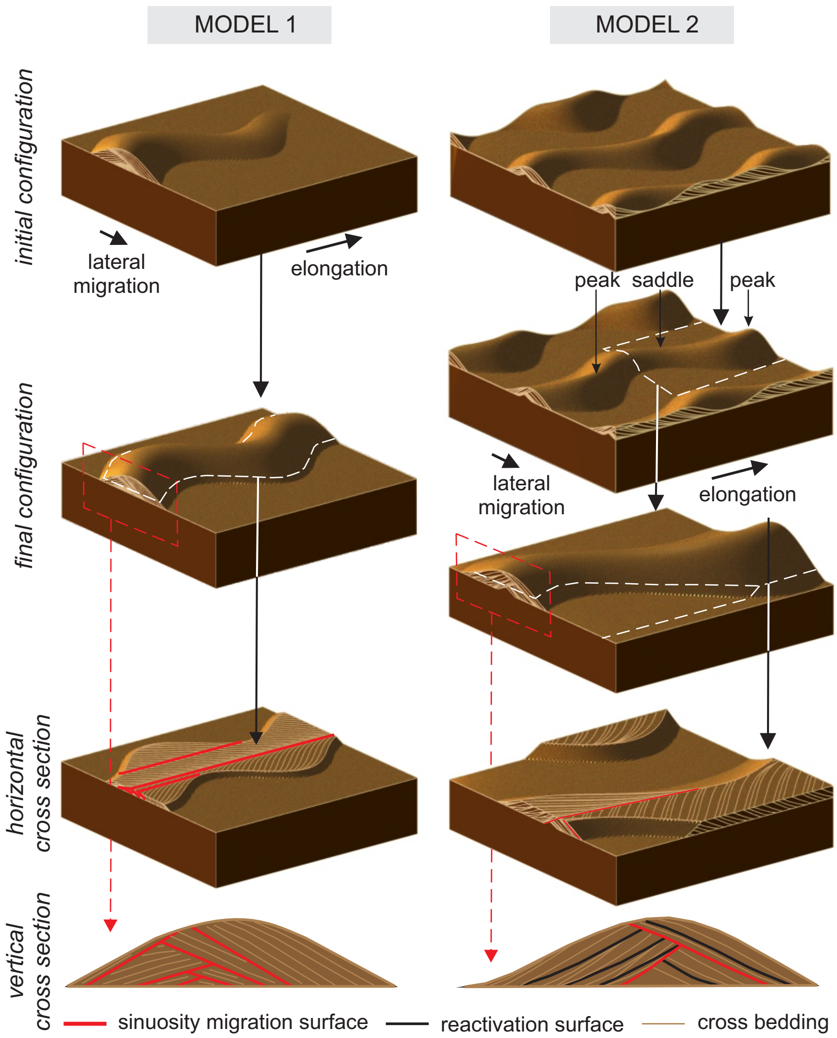

Figure 11

Argüello Scotti and Veiga

(full page width 170 mm x 154 mm)

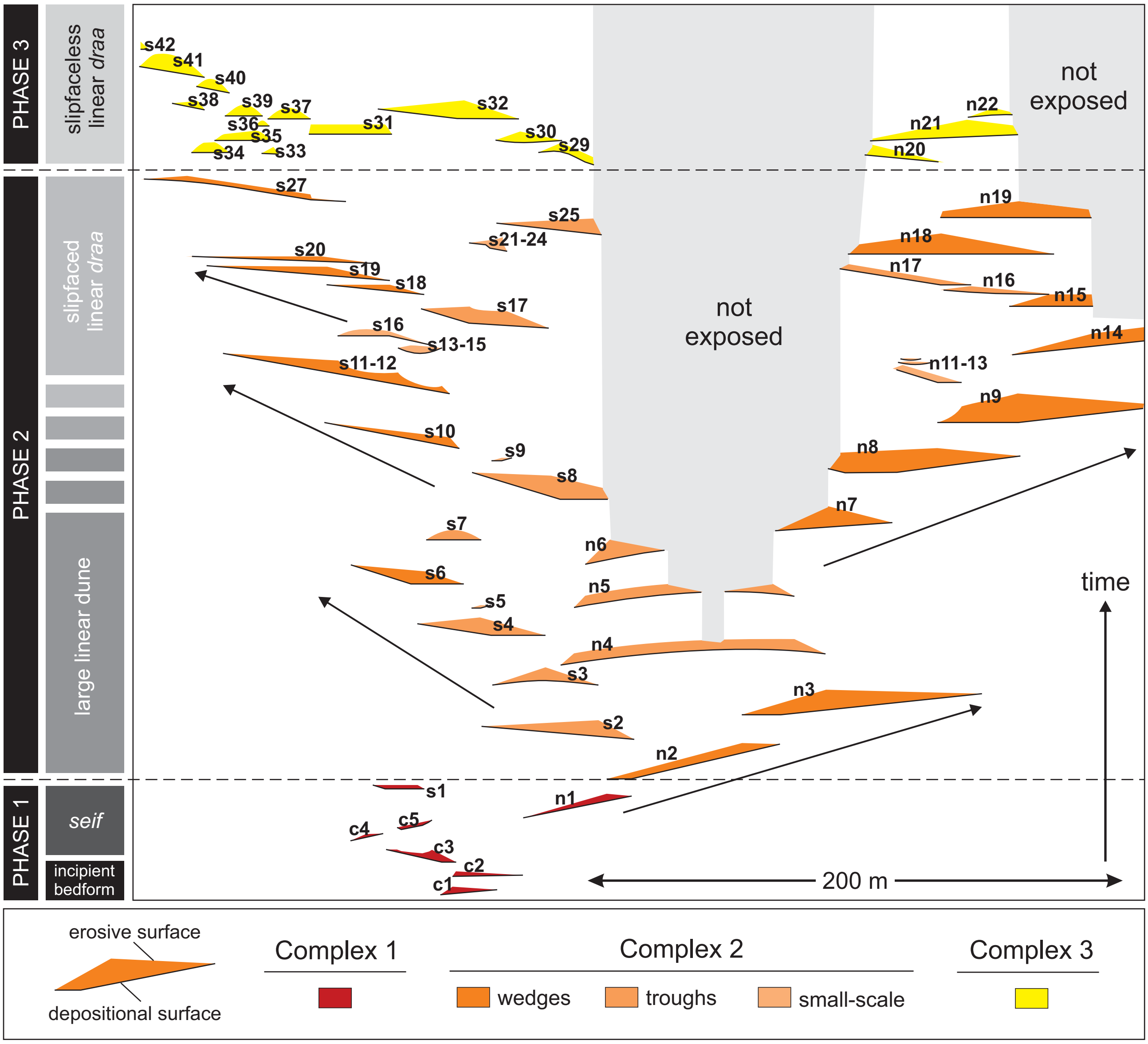

Figure 12
Argüello Scotti and Veiga
(full page width - 170 mm x 51 mm or 2/3 of a page)

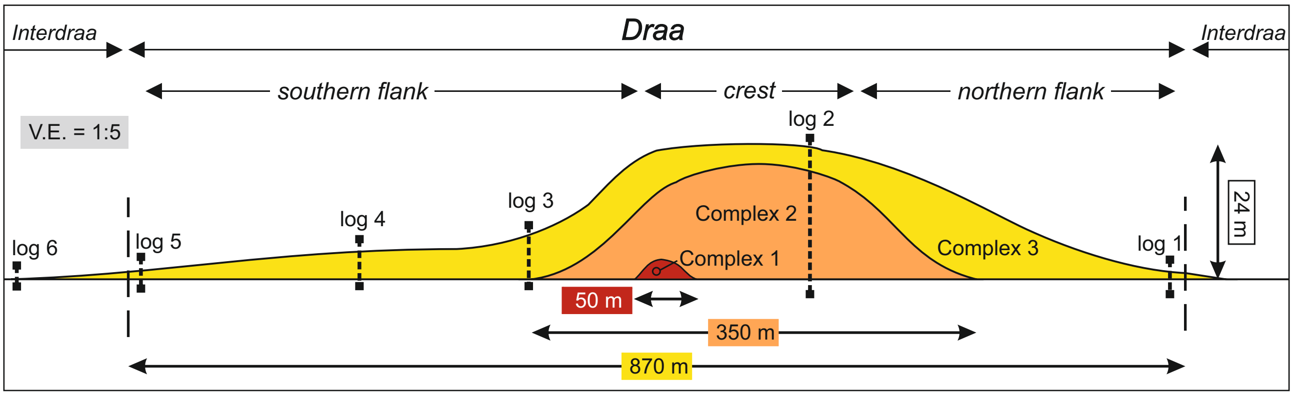

Figure 13
Argüello Scotti and Veiga
(2/3 page - 112 mm x 195 mm or 1 column width)

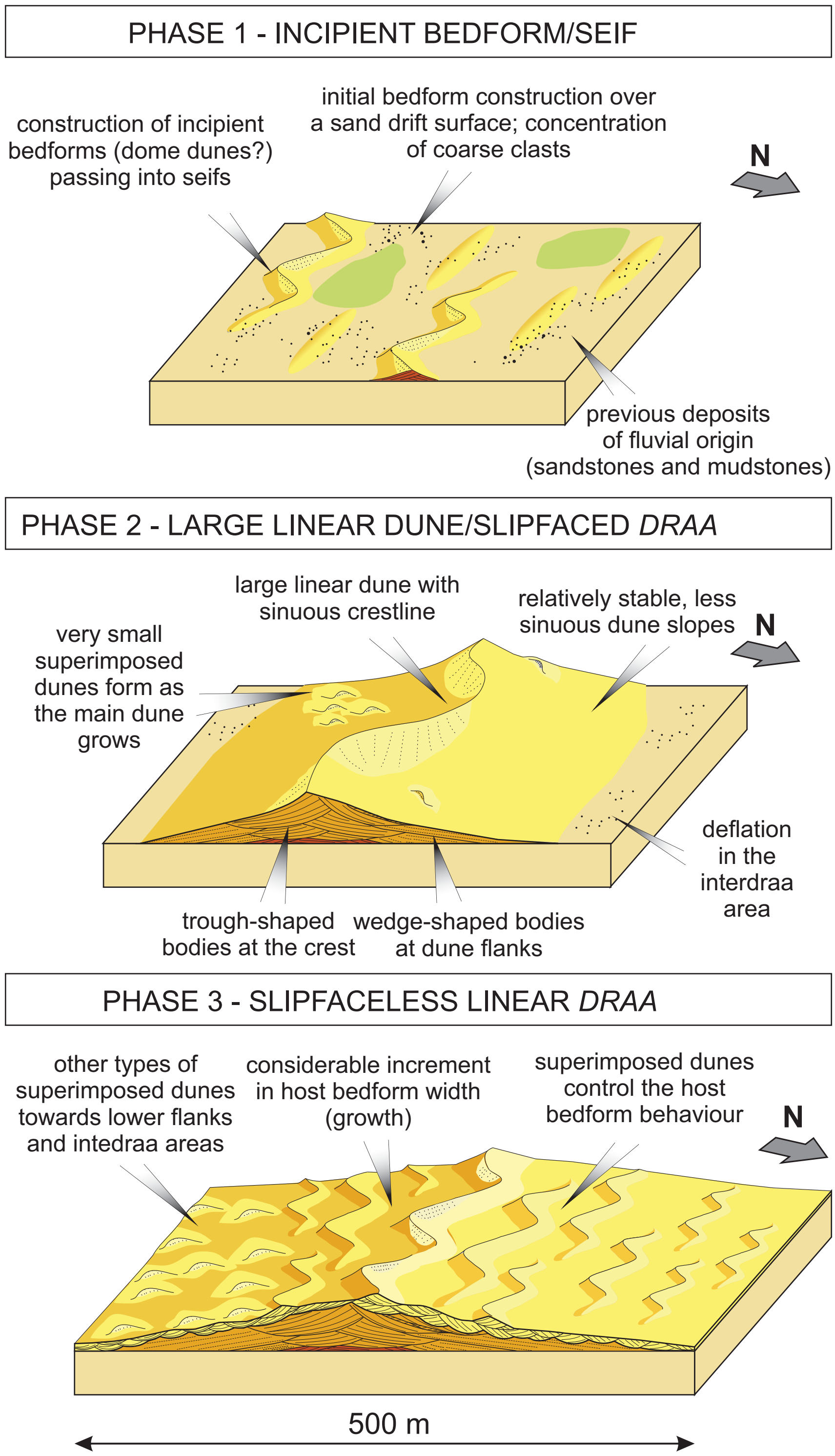

Figure 14

Argüello Scotti and Veiga

(2/3 page - 170 mm x 57 mm)

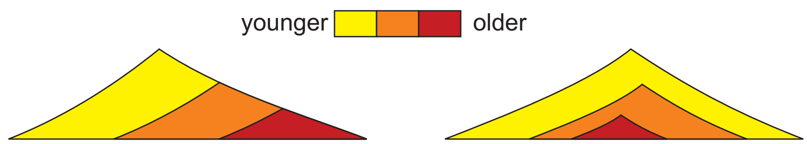

asymmetric	concentric
one flank preserved	both flanks preserved
unimodal cross bedding and oblique to unimodal bounding surfaces dip-directions	bimodal (not bipolar) cross bedding and bounding surfaces dip-directions
sustained lateral migration	growth, accretion (accumulation), long-term longitudinal dynamics
conditions more favorable for accumulation	conditions less favorable for accumulation